

MULTIPHYSICS ANALYSIS OF A CW VHF GUN FOR EUROPEAN XFEL

G. Shu*, H. Qian, S. Lal, H. Shaker, Y. Chen, F. Stephan, DESY, Zeuthen, Germany
 *on leave from IHEP/CAS, Beijing, China

Abstract

R&D for a future CW operation mode of the European XFEL (E-XFEL) started after the successful commissioning of the pulsed mode. For the electron source upgrade, a fully superconducting CW gun is under experimental development at DESY in Hamburg, and a normal conducting (NC) CW gun is under physics design at the Photo Injector Test facility at DESY in Zeuthen (PITZ) as a backup option. Based on the experience of the LBNL 185.7 MHz gun, PITZ designed a 216.6 MHz gun with increased the cathode gradient and RF power of 28 MV/m and 100 kW, respectively, to further improve the beam brightness. In this paper, the multiphysics analysis investigating the RF, thermal and mechanical properties of the NC CW gun are presented.

INTRODUCTION

Driven by the user experimental requirements, a future upgrade of the E-XFEL towards to CW operation has been proposed [1-2]. For the electron source upgrade, one option is a superconducting RF gun, which is under experimental verification at DESY Hamburg [3]. The other option is a VHF band NC CW RF gun which has demonstrated high brightness, high repetition rate (MHz-class) beam at LBNL in the APEX project [4]. Based on the APEX gun experience, a VHF band NC CW RF gun resonating at 216.6 MHz is under physical design stage at PITZ as a backup solution for the SRF gun. To further improve the beam brightness the cathode gradient and cavity voltage were pushed to 28 MV/m and 830 kV, respectively, yielding an average power loss of 100 kW.

The aim of this paper is to evaluate the cooling scheme for the PITZ CW gun to avoid excessive structural temperature, stress, and deformation. In addition, the predicted frequency shift due to heat expansion and air pressure can give a hint for the coarse tuning in the machining phase.

METHODOLOGY

The CST Microwave Studio (MWS) [5] in combination with the CST Mphysics Studio (MPS) were used to perform the coupled electromagnetic-thermal-structural finite element analysis to characterize the cooling capability of the water channels. The methodology of multiphysics simulations is described in Fig. 1. We start from the eigenmode solver in the MWS to obtain the RF induced surface heating distribution. Then, the field map is transferred into the MPS thermal module to evaluate the steady-state temperature distribution. Afterwards, the thermal simulation results are imported into the MPS structure module to simulate the heat induced expansion, i.e. the structure deformations and

the von Mises stresses. In the last step, the resonant frequency is calculated again with the deformed shape in the MWS to estimate frequency detuning due to thermal load and vacuum pressure.

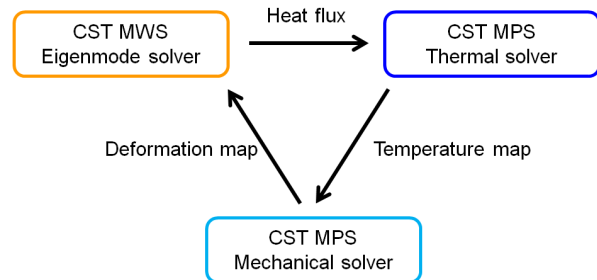


Figure 1: Schematic of the multiphysics simulations.

RF SIMULATION

The 6th sub-harmonic of 1.3 GHz (216.6 MHz), which is higher than the resonant frequency of the APEX gun (185.7 MHz), was selected as resonant frequency for better compatibility with the existing E-XFEL timing system. To improve the beam quality, the cathode gradient and the cavity voltage were enhanced to 28 MV/m and 830 kV, respectively. The cavity shunt impedance was optimized to minimize the heating load to ~100 kW in the gun. By adopting the Rogowski profile, the surface peak electric field was restricted to 2.0 Kilpatrick limit under the consideration of breakdown risk. More details about the RF design can be found in Ref. [6].

Figure 2 shows the RF model in the multiphysics simulations. The vacuum model consists of a re-entrant cavity, 90 vacuum conduction slots and a pump chamber. Figure 2 also indicates the heating distribution on the inner surface and the power dissipation on the sub-assemblies. The total power loss on the cathode nose cone is 36.2 kW with a peak surface loss density of 36.6 W/cm², which can be further reduced by elongating the nose cone. The RF heating on the rear plate, cylinder wall and the anode plate are 25.2 kW, 14.7 kW and 23.9 kW, respectively.

* guan.shu@desy.de

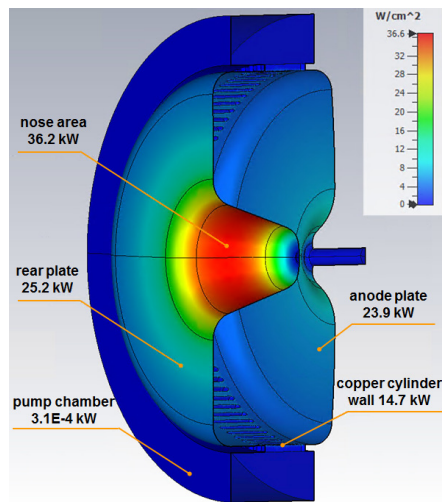


Figure 2: RF heating distribution on the inner surface and the total power dissipation on the sub-assemblies.

THERMAL ANALYSIS

Based on the APEX gun experience [7], the preliminary mechanical design of the PITZ CW gun was conducted to estimate the gun performance at full power operation. The metal body in the mechanical simulations is composed of a stainless steel pump chamber, a copper cavity and four stainless steel tuning rods (see Fig. 3). The inner water channels revealed in Fig. 3 were organized according to the heat flux map. The sub-assemblies are machined individually and jointed together by electron beam welding. All the sub-assemblies of the cavity are made by hard copper except for the cathode nose cone and the rear plate. A vacuum furnace brazing process has to be implemented to embed the cooling channels into the nose cone turning the hard copper to annealed copper.

The RF sealing is realized by a canted spring located between the copper wall and the anode plate. The tight connection surrounding the spring must be maintained by the external reinforcements. Otherwise, a gap might appear to degrade the cavity quality factor thus increasing the heat load and forming a virtual vacuum leak.

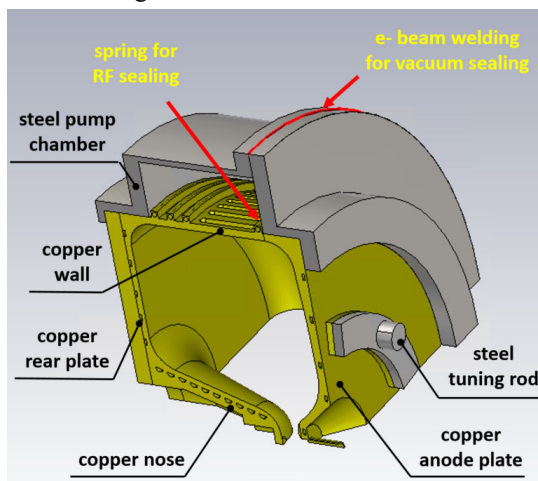


Figure 3: 3D 1/4 model in the mechanical simulations.

In order to simplify the simulation, the non-critical components (e.g. bolts, flanges, supports and external reinforcements) are not included in the model. The nonlinearity of the material properties are not taken into consideration in the thermal simulation. The ambient temperature is considered to be 20°C.

The RF heating is removed by water with a constant temperature of 20°C at a speed of 3 m/s. The water temperature rise distribution in the channel will be complemented in the future work. The cooling parameters used in the thermal simulation are listed in Table 1. The heat convection factors determined by the water velocity, cooling pipe dimensions and water temperature are derived from the empirical formulas [8].

Table 1: Cooling Parameters of the Water Pipes in the Thermal Simulation

Cooling parameters	Water speed [m/s]	Flow rate [L/min]	Heat convection factor [W/(m²K)]
Anode plate	3	7.2	12757.5
Cylinder wall	3	9.0	11927.2
Rear plate	3	7.2	12757.5
Cathode nose cone	3	10.2	12137.0

Figure 4 depicts the steady-state temperature distribution in the cavity body at 100 kW power loss yielding a maximum temperature of 57.2°C located near the center of the anode nose cone. The cathode temperature is 45°C which is compatible with various photocathodes e.g. Cs₂Te and CsK₂Sb [9].

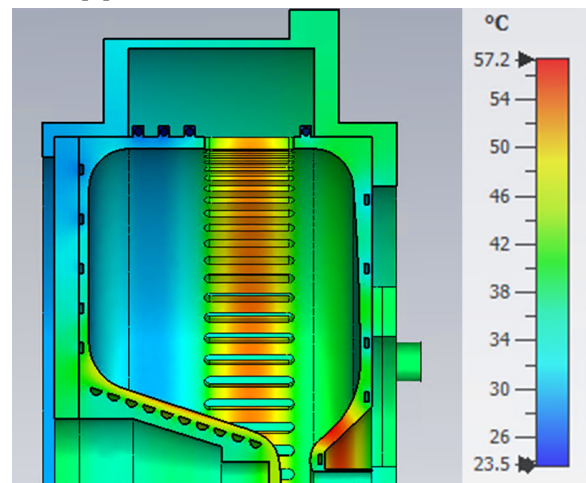


Figure 4: Temperature distribution with 100 kW power dissipation on the cavity wall.

STRUCTURE ANALYSIS

For the structure simulation, the thermal results were imported into the MPS mechanical module. Vacuum pressure was applied to the inner surface as a counteracting force suppressing the thermal expansion. As mentioned in the previous section, the connection between the anode plate and the copper wall is of great importance. Therefore, we fixed the areas related to the electron beam welding line (Fig. 3) in simulations.

Content from this work may be used under the terms of the CC BY 3.0 licence (© 2019). Any distribution of this work must maintain attribution to the author(s), title of the work, publisher, and DOI

The deformation map due to the thermal expansion and inside vacuum pressure is shown in Fig. 5. The maximum displacement is 0.26 mm located at the middle of the anode plate. The equivalent von Mises stress distribution is shown in Fig. 6. The peak stresses in the soft copper, hard copper and the steel chamber are 45.0 MPa, 110 MPa and 114 MPa, respectively. The stresses are much lower than the yield strength of the corresponding materials [10]. In addition, the fixed boundary means the displacement is set to zero mandatorily which overestimates the stress level around the fixed areas.

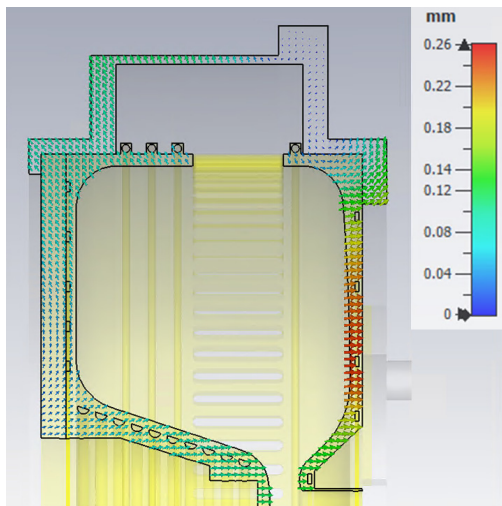


Figure 5: Cavity displacement distribution.

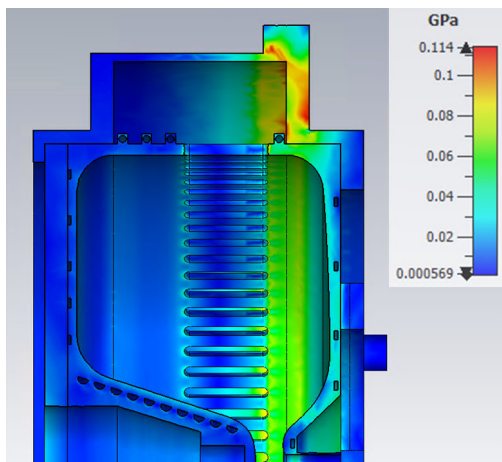


Figure 6: Cavity von Mises stress distribution.

FREQUENCY TUNING APPROACH

Without frequency tuning, the cavity frequency changes under different conditions. From room temperature frequency in the air to the frequency under full power operation, the frequency change is defined by the vacuum pressure induced cavity deformation, air permittivity and thermal expansion. According to the simulations, the frequency is reduced by 262.4 kHz due to the vacuum pressure induced deformation. The 100 kW thermal expansion yields a frequency increase by 206.2 kHz. The frequency is increased by 66.9 kHz due to the air permittivity (here we

assume the air temperature is 20°C, the relative humidity is 40% and the atmospheric pressure is 101 kPa). From the status in the air to the operation condition, the total frequency change is 10.7 kHz. From the cavity off in vacuum to the full operation, the total frequency shift is +206.2 kHz.

It has been found for the APEX gun that the anode temperature has a significant impact on the cavity frequency. Figure 7 shows the dependence of the water heat transfer coefficient and the frequency shift on the anode cooling flow. The frequency can be increased by ~400 kHz with the flow reducing from 9.2 L/min to 1.2 L/min. Simulations indicate the stresses with this anode water flow range are less than the material yield limits. The ‘cut and try’ technique will be used for the coarse tuning in the machining stage. The anode temperature tuning and four external tuners can be used for the fine tuning. The large temperature tuning range can ease the machining precision requirement and reduce the tuner range requirement. The detailed mechanical design of the tuners will be performed in the next stage.

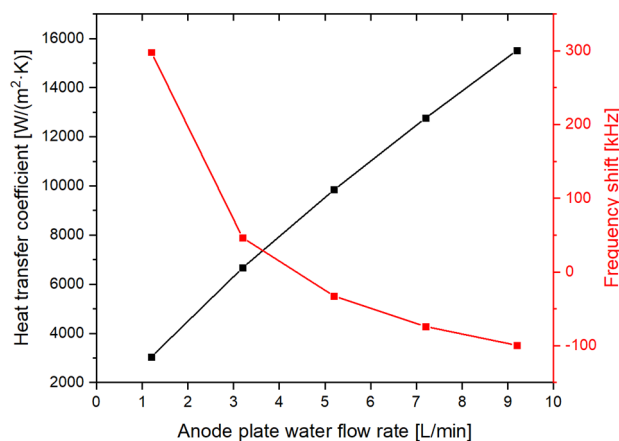


Figure 7: Dependence of the water heat transfer coefficient and the cavity frequency shift on the anode plate water flow rate.

CONCLUSION

A coupled electromagnetic-thermal-structural analysis of a 216.6 MHz NC CW RF gun for the European-XFEL was performed using the CST multiphysics package. The simulated temperature distribution in the nominal operation regime is suitable in respect to the overall physical design. The equivalent stresses are well below the material yield limits. In addition to the CST simulations, the consistent results were also obtained in the ANSYS benchmark analysis. The simulation results indicate that the designed cooling scheme has enough cooling capacity to handle ~100 kW thermal heating.

REFERENCES

- [1] J. K. Sekutowicz *et al.*, “Feasibility of CW and LP Operation of the XFEL Linac”, in *Proc. 35th Int. Free Electron Laser Conf. (FEL’13)*, New York, NY, USA, Aug. 2013, paper TUOCNO04, pp. 189-192.
- [2] R. Brinkmann *et al.*, “Prospects for CW Operation of the European XFEL in Hard X-ray Regime”, in *Proc. 36th Int.*

- Free Electron Laser Conf. (FEL'14)*, Basel, Switzerland, Aug. 2014, paper MOP067, pp. 210-214.
- [3] E. Vogel *et al.*, "SRF Gun Development at DESY", in *Proc. 29th Linear Accelerator Conf. (LINAC'18)*, Beijing, China, Sep. 2018, pp. 105-108.
doi:10.18429/JACoW-LINAC2018-MOP0037
- [4] F. Sannibale *et al.*, *PRST-AB*, 15, 103501 (2012).
doi.org/10.1103/PhysRevSTAB.15.103501
- [5] CST, <http://www.cst.com/>.
- [6] G. Shu *et al.*, "First Design Studies of a NC CW RF Gun for European XFEL", in *Proc. 10th Int. Particle Accelerator Conf. (IPAC'19)*, Melbourne, Australia, May 2019, paper TUPRB010, pp. 1698-1701.
doi:10.18429/JACoW-IPAC2019-TUPRB010
- [7] R. P. Wells *et al.*, "Mechanical design and fabrication of the VHF-gun, the Berkeley normal-conducting continuous-wave high-brightness electron source", *Review of Scientific Instruments*, 87.2 (2016): 023302.
doi:10.1063/1.4941836
- [8] F. Kreith, *The CRC Handbook of Thermal Engineering*, CRC Press, Boca Raton, 2000.
- [9] Z. Ding *et al.*, "Temperature-dependent quantum efficiency degradation of K-Cs-Sb bialkali antimonide photocathodes grown by a triple-element codeposition method", *Physical Review Accelerators and Beams*, 20.11 (2017): 113401.
doi:10.1103/PhysRevAccelBeams.20.113401
- [10] MakeItFrom.com,
<https://www.makeitfrom.com/material-group/Copper-Alloy>